VIABILITY OF A MAGNETIC ACTUATOR IN LATERAL SECONDARY SUSPENSION OF INDIAN RAIL VEHICLE

[1]Ram Rakshit Rustagi, [2]Tejbir Kaur
[1]M.tech Student, [2]Assistant Professor
[1]Department of Mechanical Engineering,
[1]Punjab Engineering College, Chandigarh, India

Abstract: Magnetic Actuators are in active usage to attenuate vibrations. This paper depicts the practicality of the use of magnetic actuator in the lateral secondary suspension of (LHB-FIAT) rail vehicle of Indian Railways which consequently ameliorates ride comfort. As temperature is an imperative parameter for the actuator's performance, force convection is requisite to disperse heat adequately. In order to determine the air current at the actuator's location a 3-D model of the rail vehicle is generated and the same is simulated at low, medium and high speeds ranging from 60-200 km/h in Ansys-Fluent. Further, Transient Thermal examination of 2-D model of the actuator is done in Ansys-workbench to identify the variation of temperature within the actuator itself.

Index Terms - Magnetic actuator, Lateral Secondary suspension, Fluent Analysis, Transient Thermal Analysis

I. INTRODUCTION

With the expanding utilization of railroad vehicles in the world numerous nations have found a proclivity towards increasing speed and ride comfort of trains. Be that as it may, expanding train speed causes noteworthy vibration issues, which decreases the ride comfort and operational safety and increment track maintenance costs. [1] The prominent source of vibrations are the unevenness and the irregularities in the tracks. [2] The vibrations that are produced from the irregularities are firstly transferred to the bogie through primary suspension and later to the car body through secondary suspension.

To attenuate vibrations many researchers have presented various methods and control strategies for vibration reduction. Hydraulic actuators are easy to install [3, 4] but oil leakage problems persists [5, 6]. Pneumatic actuators have also been in practiced but have low frequency bandwidth [7, 8]. MR dampers have also find a place in the to ameliorate ride comfort as they require less power and are cheaper but the force is directly dependent on the velocity. Moreover corrosion problem and regular maintenance is required. As far as Indian Railways is considered Sharma et al. [9] has found an application of MR damper vertical secondary suspension using Linke Hofmann Busch (LHB) and Fabbrica Italiana Automobili Torino (FIAT) LHB-FIAT configuration and found an amelioration of ride comfort of a significant amount. As far lateral vibration is concerned Jun-Ho Yoon et al. [10] have designed and optimized a Tubular Permanent Magnet Actuator (TPMA) which do not require continuous power, intricate control, or any fluid [11].

From further study it was found that as the operating temperature of the electromagnetic actuator increases, the life of the insulator decreases. If the actuator constantly operates above the maximum allowable temperature, it causes a thermal problem and the actuator will not operate [12]. The maximum temperature in the coil decreased exponentially with air velocity. It was confirmed that air velocities from 3 m/s to 10 m/s substantially affected the thermal performance but enhancement of air cooling was diminished at air velocities higher than 10 m/s.

As the air current around the actuator is a critical parameter that decides the performance of the actuator thus, this paper focuses on the fluent analysis at various operating speed of the coach. The viability of the magnetic actuator in Indian Railways can be checked in three stages i.e. geometric constraints, fluent analysis to evaluate air current and thermal analysis to validate the geometric constraints. The total length of the actuator used is around 1 m and the space available between the central axis and the position of the secondary springs is around 1.25 m which is sufficient enough to mount the actuator. The width of the actuator is around 100mm which is more than enough to mount the actuator.

As far as fluent analysis is considered a 3-D model LHB-FIAT coach was used for air current study. The figure 1 shows the flowchart of the modelling and simulation of the coach for air current evaluation.

After the evaluation of air current at various speeds ranging from 60 to 200 km/h a 2-D transient thermal analysis of the actuator is conducted at particular sets of boundary condition so as to validate the results from the existing 3-D model results. The figure 2 depicts the flowchart for 2-D transient thermal simulation.

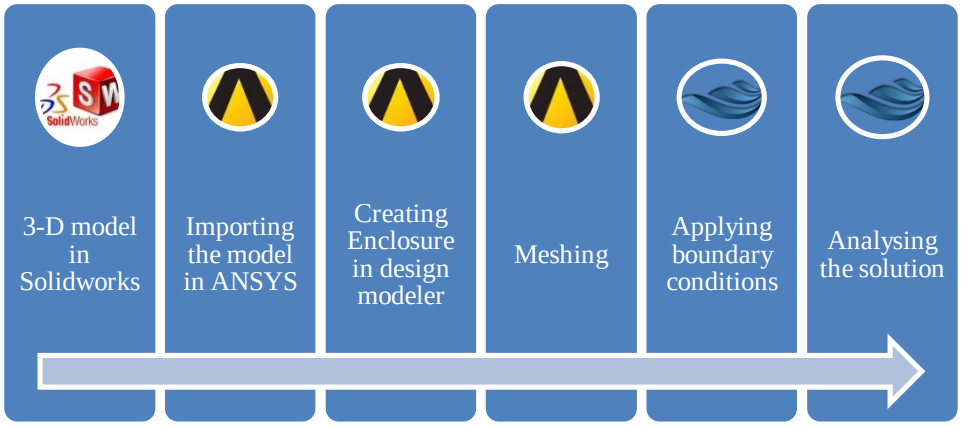

Fig. 1 Flowchart of Fluent Simulation

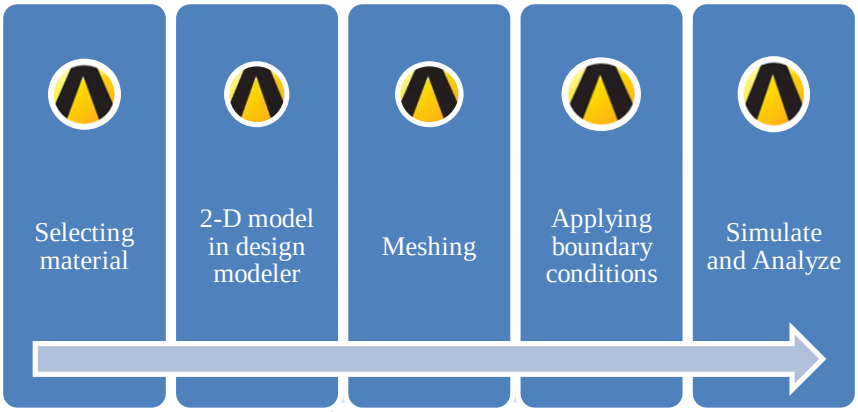

Fig. 2 Flowchart of Transient Thermal simulation

II. Modelling And Simulation

2.1 Fluent Model

A coach comprises of a car body and a bogie. A particular type of coach LHB-FIAT was used in simulation. This model is half in length as compared to the original length and half across the width as the coach is symmetric about its central plane. The bogie as well was made half as it is also symmetric. Complex parts of the bogie were neglected as it would complicate both simulation as well as meshing. Moreover, system requirements to run the simulation is of extremely high level as simulating a 14m length model is very cumbersome process. As the simulation is of steady nature so a constant speed is given to the inlet velocity. Steady state was taken because the geometry is too large and the transient analysis would need a lot of sources. So the model was tested from low speed to high speed i.e. 60, 75, 90, 110, 130, 160, 190, 200 km/h. This helped in getting results from all phases of the train travel. Figure 3 shows the solidworks model created by using sketch tracing and surfacing. Table 1 and 2 shows sets of dimensions that were used in creating 3-D model of coach.

The model generated was imported in ANSYS and enclosure was formed around the coach so that air has a medium to travel. There were assumptions that were considered while performing fluent analysis. While giving the inlet area to the air the area below the bogie was neglected as for a long train the air current coming from straight across the bogie will lose its energy, thus was neglected. Moreover, complex parts of the bogie were neglected. Springs were used as a solid cylinder. The air flow was studied for the steady state. The simulation was based on pressure gradient. A turbulency of 5% was used for the analysis.

Table 1 Dimensions of various parts of LHB car body

Part	Dimension (m)
Overall length	24000
Width of car body	3240
Distance between bogies	14900
Overall height of the coach	4039
Height of bogie	1320
Distance of bogie from edge of coach	4550

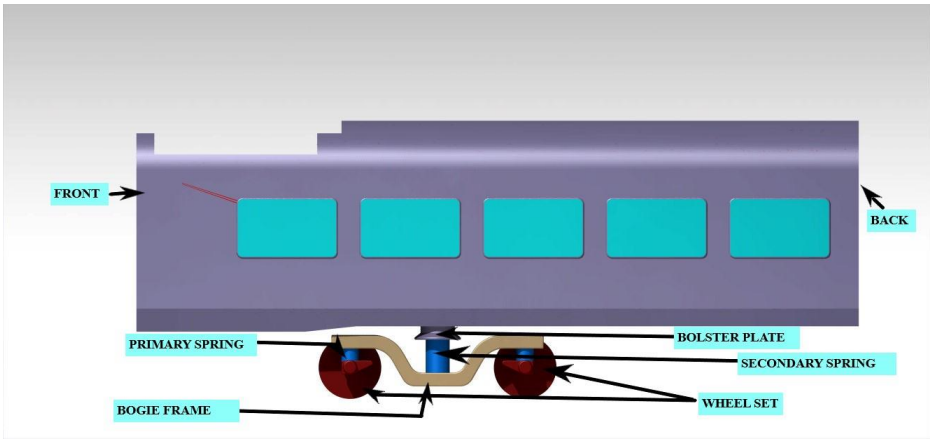

Fig. 3 Surface model of the LHB-FIAT coach

Table 2 Technical data of FIAT bogie

Part	Dimension (mm)
Axle distance	2560
Diameter of new wheels	915
Diameter of max. worn wheel	845
Distance between the wheels	1600
Brake disc diameter	640
Bogie width	3030
Bogie length	3534
Bogie weight	6300 Kg

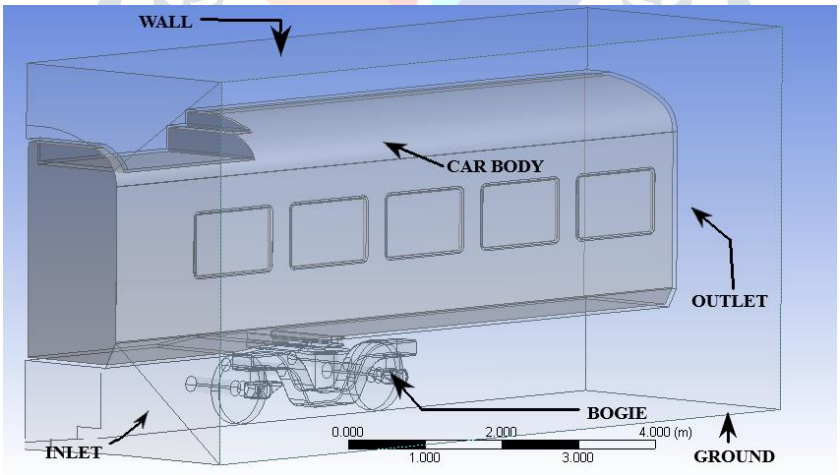

Fig. 4 Isometric view of Coach showing various parts of enclosure as well as coach

The figure 4 gives the glimpse of the coach in an isometric view featuring inlet, outlet carbody, bogie and enclosure.

A mesh breaks space into components (or cells or zones) over which the conditions can be comprehended, which at that point approximates the arrangement over the bigger area. Component limits might be obliged to lie on inside or outside limits inside a model. Higher-quality (better-formed) components have better numerical properties, where what comprises a "superior" component relies upon the general overseeing conditions and the specific answer for the model example.

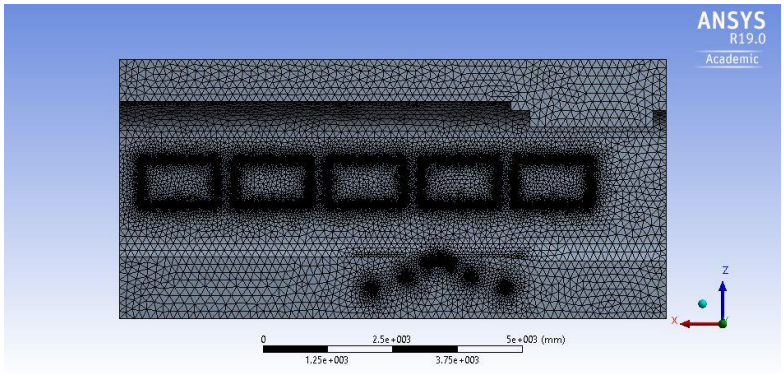

(a)

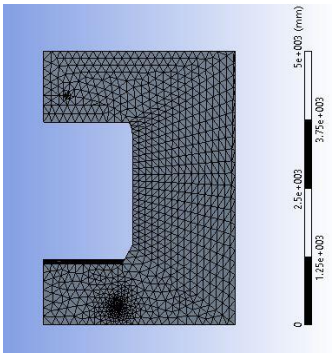

(b)

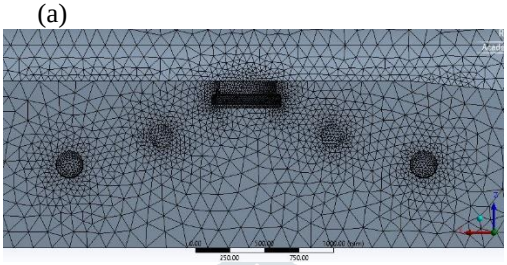

(c)

Fig. 5 Meshing of carbody (a) side view (b) front view and (c) bogie component

In the simulation since a lot of complexity was faced in the model so making tetrahedral elements was a good option for one since these elements are good for complex shapes. Small element size was given near the bogie portion as the air current velocity should be very close to actual value. The inlet of the enclosure was broken down into pieces so as to mesh it meticulously.As far as mathematical model is considered a standard k-ε was used as the simulation is done for the calculation of air current study. Since, the drag and lift forces were not the part of the simulation so a standard model had solved the purpose. Two-condition choppiness models permit the assurance of both, a fierce length and time scale by illuminating two separate transport conditions. The standard model in ANSYS Fluent falls inside this class of models and has turned into the workhorse of useful designing stream estimations in the time since it was proposed by Launder and Spalding. Power, economy, and sensible precision for a wide scope of violent streams clarify its notoriety in modern stream and warmth exchange reproductions. It is a semi-exact model, and the induction of the model conditions depends on phenomenological contemplations and observation.

The standard k - ε model is a model dependent on model transport conditions for the choppiness dynamic vitality (k) and its dissemination rate (ε). The model transport condition for k is gotten from the accurate condition, while the model transport condition for ε was acquired utilizing physical thinking and looks to some extent like its scientifically precise partner.

The choppiness motor vitality, k, and its rate of dispersal, ε, are gotten from the accompanying transport conditions:

$$\frac{\partial}{\partial t}(\rho k) + \frac{\partial}{\partial x}(\rho k u_i) = \frac{\partial}{\partial x_j}\left[\left(\mu + \frac{\mu_t}{\sigma_k}\right)\frac{\partial k}{\partial x_j}\right] + G_k + G_b - \rho\varepsilon - Y_M + S_k \quad (2.1)$$

And

$$\frac{\partial}{\partial t}(\rho \varepsilon) + \frac{\partial}{\partial x}(\rho \varepsilon u_i) = \frac{\partial}{\partial x_j}\left[\left(\mu + \frac{\mu_t}{\sigma_k}\right)\frac{\partial \varepsilon}{\partial x_j}\right] + C_{1\varepsilon}\frac{\varepsilon}{k}(G_k + C_{3\varepsilon}G_b) - C_{2\varepsilon}\rho\frac{\varepsilon^2}{k} + S_\varepsilon \quad (2.2)$$

G_k = turbulent kinetic energy, G_b = turbulent kinetic energy due to buoyancy, $C_{1\varepsilon}$, $C_{2\varepsilon}$ and $C_{3\varepsilon}$ are constants, σ_k and σ_ε are the turbulent Prandtl numbers for k and ε

2.2 Transient Thermal Model

After the implementation of the fluent analysis, we move one step forward towards the transient thermal analysis. This is done to validate the design geometry of the actuator. As the researchers have done transient thermal analysis on a one sixth model, this analysis will be done on a 2-D model. This will help in validating the same results by putting the same boundary conditions as applied by (Yoon et al.) to a one sixth model.

First step of the simulation is to select different materials required for the simulation. If the material is not available, ANSYS has a feature to create a new one. After selecting appropriate material, 2-D model is generated in design modeler. After that various connections at the interface of the various parts and break down the geometry is broken down into smaller elements, so as to implement the transient thermal model for simulation. Fourth step is to provide boundary conditions, each time step and for how long one wants to run the simulation. Finally the simulation is run and the results are analyzed.

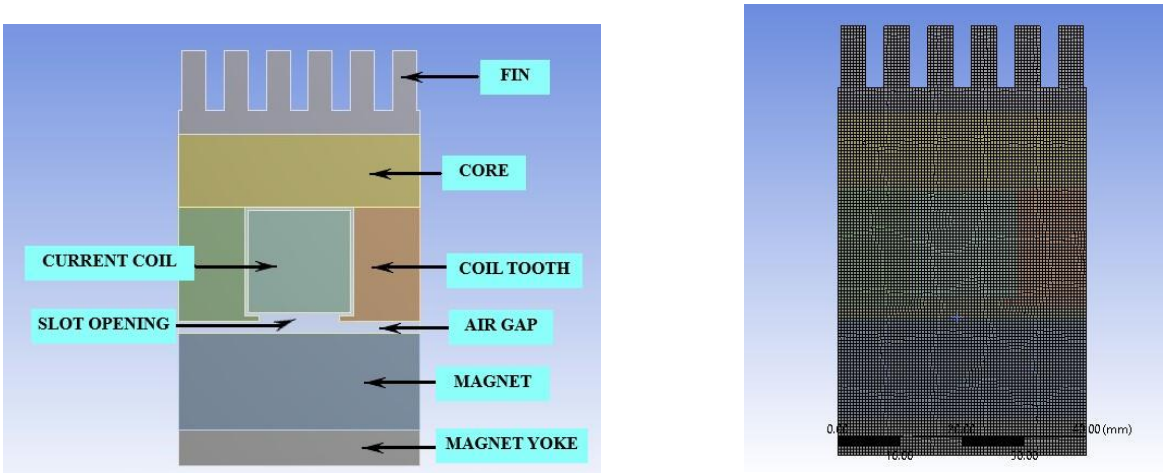

(a) (b)

Fig. 6 Section of 2-D actuator for thermal Analysis (b) Meshing of 2-D actuator

The source of heat is the copper coils, so heat will get dissipate through teeth/-coil, core and later through the fin. Since, the simulation will be based on the particular set of boundary conditions, so the heat convective coefficient at the fins is 38 W/m^2K for air current 8m/s. The temperature of the coils is the input parameter and given such that the coil reaches the maximum operating temperature of 130°C. This simulation deals with the study of the variation of the temperature throughout the actuator under working conditions.

There are many ways to mesh geometry. Since, the geometry is simple, 2-D and does not contain any intricate parts it was good to use mapped face meshing that mapped quadrilateral elements to the geometry. This helped me in generating a beautiful mesh.

The quality of the mesh plays a significant role in the accuracy and stability of the numerical computation. Regardless of the type of mesh used in your domain, checking the quality of your mesh is essential. To judge the quality of mesh there are many ways such as Skewness, Orthogonal quality and Aspect ratio.

Table 3 Mesh quality for transient thermal analysis

Parameter	Recommended	Achieved
Skewness	**0**	**0.0010384**
Orthogonal Quality	**1**	**0.99979**
Aspect Ratio	**1**	**1.0111**

As the magnetic analysis was not performed, the source temperature of the copper coil was calculated by the survey. The general equation of the temperature for the coil is a saturation curve.

$$T = \frac{aX}{b+X} + 20 \qquad (2.3)$$

Where T is the temperature in (°C) and X is the time in hours.

Since, the simulation was run for 1.5 hours so for T = 130°C, X = 1.5 hours is the first boundary condition for calculating the constants 'a' and 'b'. Second boundary condition was evaluated from the graph of the survey. At T = 127°C, X = 0.5 hours.

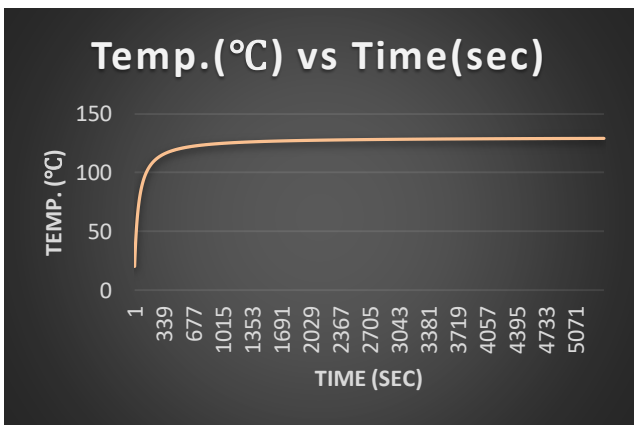

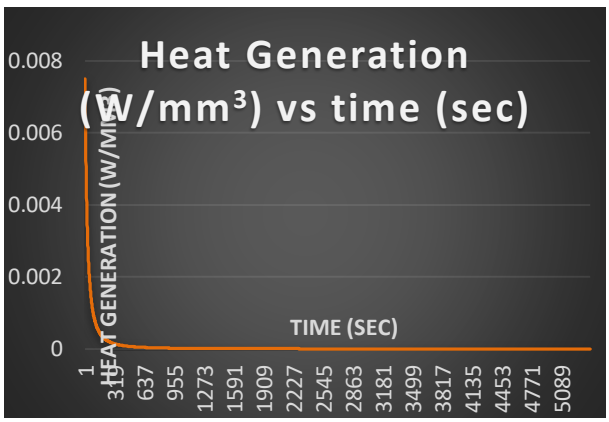

(a) (b)

Fig. 7 (a) Temperature profile of copper coil (source) and (b) Heat generation in copper coil

Since, the heat is also generated in the copper coil which will be transferred to the surface of the actuator and convective forcefully.

$Q_{gen} = \rho c \Delta T$ (2.4)

Where ρ = density kg/m^3, c = specific heat J/KgK, ΔT is the temperature difference.

Here,Q_{gen} is in J

Rate of heat generation is $q_{gen} = \rho c \frac{\Delta T}{dt}$ (2.5)

Since, $T = \frac{aX}{b+X} + 20$ (2.6)

Therefore, $\frac{\Delta T}{dX} = \frac{a(b+X) - aX}{(b+X)^2}$ (2.7)

This implies, $\frac{\Delta T}{dX} = \frac{ab}{(b+X)^2}$ (2.8)

Thus, $q_{gen} = \rho c \frac{ab}{(b+X)^2}$ (2.9)

Where $\mathbf{q_{gen}}$ is in W/m^3. The final relation on substituting the values of ρ and c as 8933 kg/m^3 and 385 J/kgK respectively is:

$$q_{gen} = \frac{8933*385*a*b}{3600*10^9*\left(\frac{b}{3600}+X\right)}$$ 2.10

Now, q_{gen} is in W/mm^3

After getting the values of 'a' and 'b' from the temperature equations, the value of heat generation is evaluated and used as a boundary condition for the analysis.

Since the interface is made up of two different materials so there will be the presence of micro air gaps leading to thermal contact resistance. Thus, the above table lists the various interfaces and thermal contact resistance for each interface. Table 4 shows the conductivity, specific heat and density of the various materials used in the simulation.

Table 4 Thermal Properties of various materials used in Thermal Simulation

Material	Conductivity (W/m-k)	Specific Heat (J/kg-k)	Density (kg/m3)
Air	0.0263	1007	1.1614
Copper	400	385	8933
Silicon Steel	24.2 (r direction)	446	7650
	5.0 (z direction)		
Aluminium	210	900	2700
NdFeB	6.5	460	7600
Coil-core interface	0.1		
Stator- mover interface	0.15		
Core- housing interface	0.3		

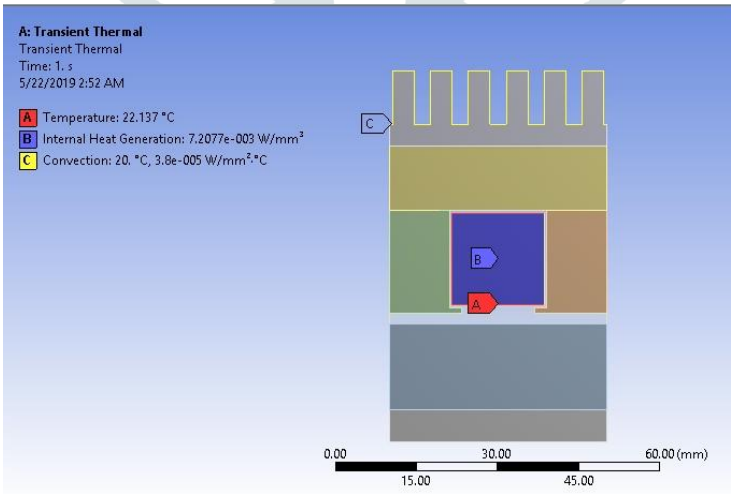

Fig. 8 Boundary conditions for transient thermal

The figure 8 shows the final boundary conditions applied for the transient thermal analysis of 2-D section of the actuator.

III. RESULTS

As known from the survey temperature plays a critical role in the performance of the actuator, so forced convection was needed to dissipate heat effectively for which speed ranging from 3-10 m/s gave an appreciated result. Since, the place of

positioning of the actuator is at 4.4 m behind the front section of the coach on the longitudinal axis defined by X-axis in the simulation. Thus, the model was clipped at 4.4 m so as to give the glimpse of the velocity variation virtually.

The total length of the simulated model is 10.555 m (in x direction) but the actuators position is at 4.4m so the figure above shows the volume rendered region beyond 4.4m so that things can be seen visually as well. The figure 5.1(c) represents the behaviour of the air current while passing the vicinity of the coach.

The length of the actuator is 0.9m. To measure the velocity at the throughout the length of 0.9m a probe was taken and was used to measure it at an increment of 0.025m in y direction i.e. the direction of the actuator. The position of the actuator from the ground is at a position of 0.65m, so z=0.65m. x and z co-ordinates are fixed and y co-ordinate is changed incrementally.

Since, the simulation was done for a range of 60-200 km/h thus a lot of images were produced. But for now only few images will be shown.

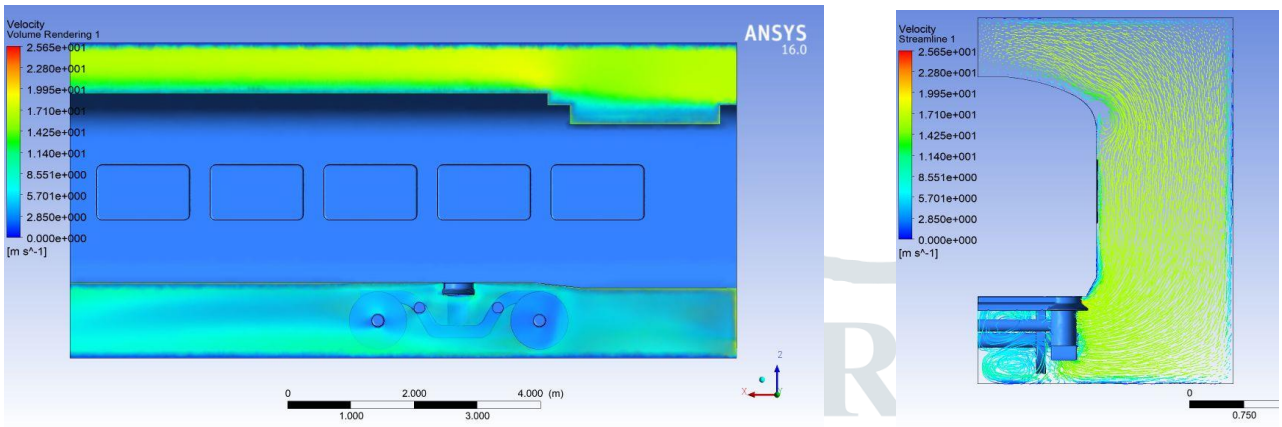

(a) (b)

Fig. 9 (a) Velocity profile around the coach (60 km/h)-side view and (b) Stream flow around actuator in the clipped section

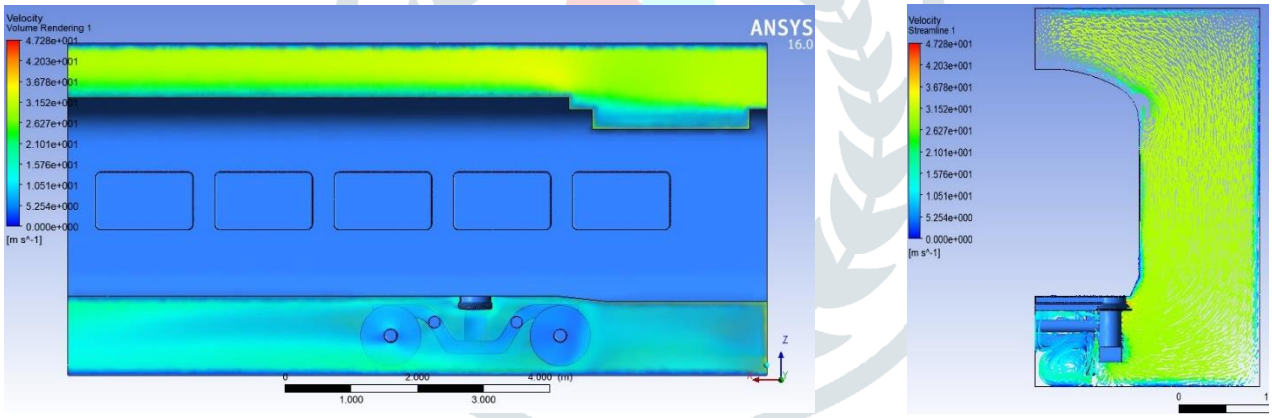

(a) (b)

Fig. 10 (a) Velocity profile around the coach (110 km/h)-side view and (b) Stream flow around actuator in the clipped section

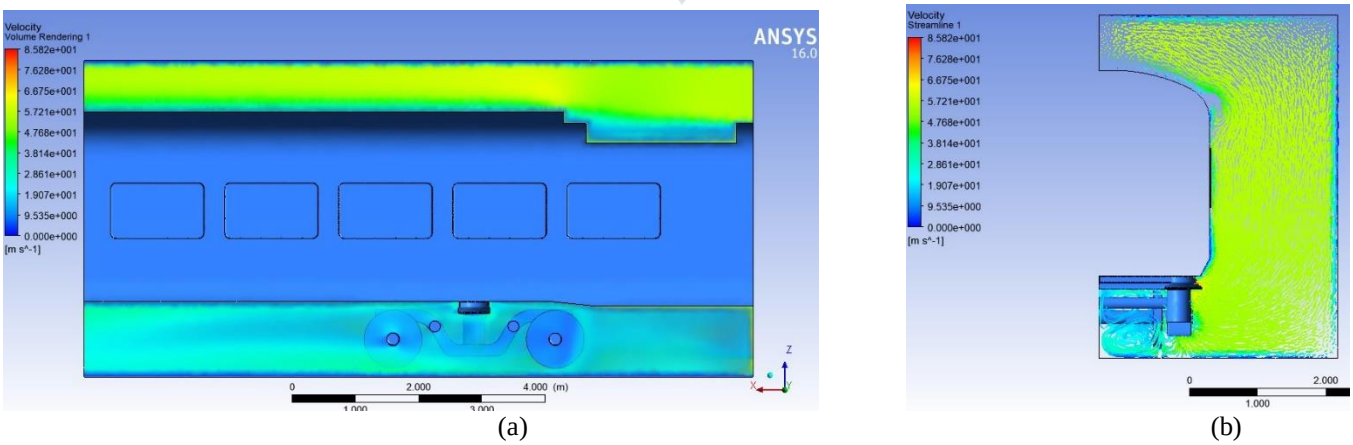

(a) (b)

Fig. 10 (a) Velocity profile around the coach (200 km/h)-side view and (b) Stream flow around actuator in the clipped section

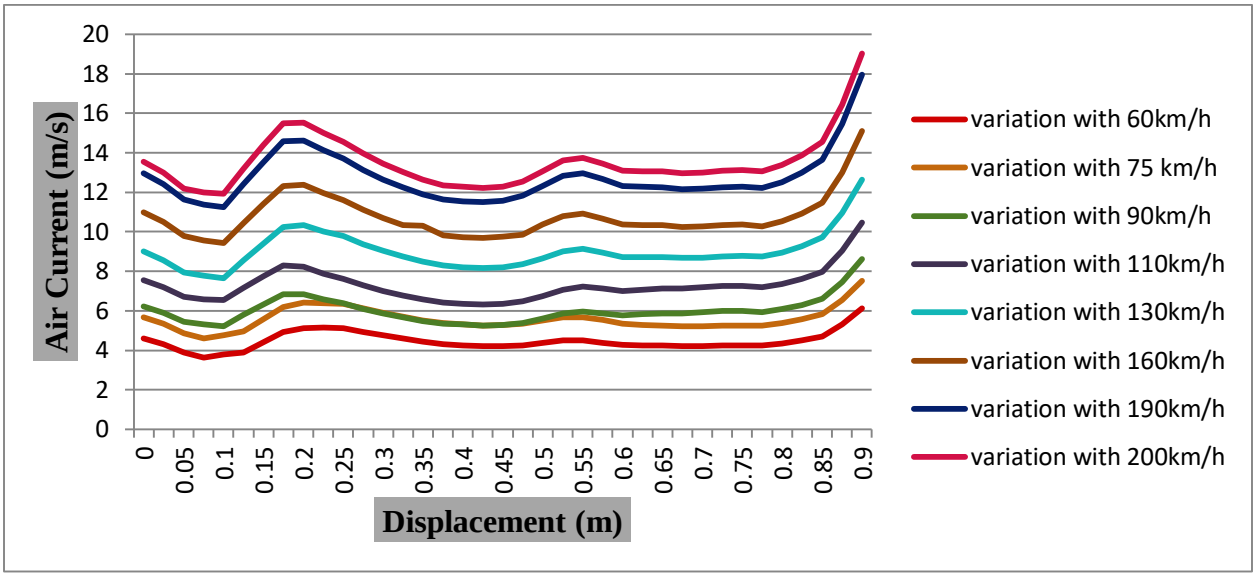

Fig. 10 Combined comparison of various air current velocities w.r.t. varying speed vs Displacement in Y-Axis

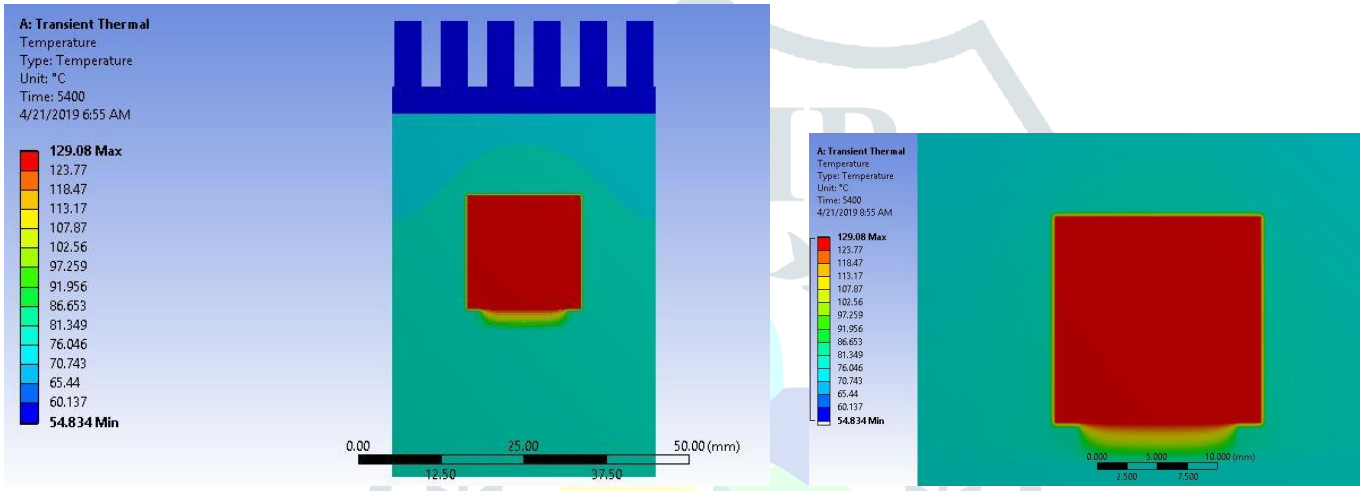

(a) (b)

Fig. 11 (a) Variation of temperature in the actuator at 5400 seconds and (b) Temperature variation around the coil

It is clear from the figure above that the maximum temperature reached by coil is 129.08℃ though the saturation comes after 130℃. The maximum temperature at the fin (at extreme location) reached a value of 54.834. One can see a sudden loss of thermal energy from core to fin housing. This is due to the fact that there is a thermal contact resistance between the fin and the core preventing the two interfaces to be at same temperature.

As the temperature in the copper coil follows a saturation curve, similar observation can be made as of coil tooth too but constants of the general graph will vary. The minimum temperature observed was 20 ℃ at time t = 0 seconds, whereas the maximum temperature reached to 81.8 ℃ at 5400 seconds. At 4316 seconds the temperature reached 80 ℃ which means for almost 1100 seconds the temperature rise was just 1.8 ℃. The variation of the temperature in the core is not as such of saturation type but in 5400 seconds it reaches to 79.056 ℃. The minimum temperature in the fin is 20 ℃ at the start of the simulation which is equal to the surrounding temperature. The maximum temperature reaches 55.236 ℃ at the end of the simulation i.e. at 5400 seconds. One can also observe for the first 100 seconds of the simulation that the temperature at the fin section follows upward parabola and after that follows saturation curve but with different constants.

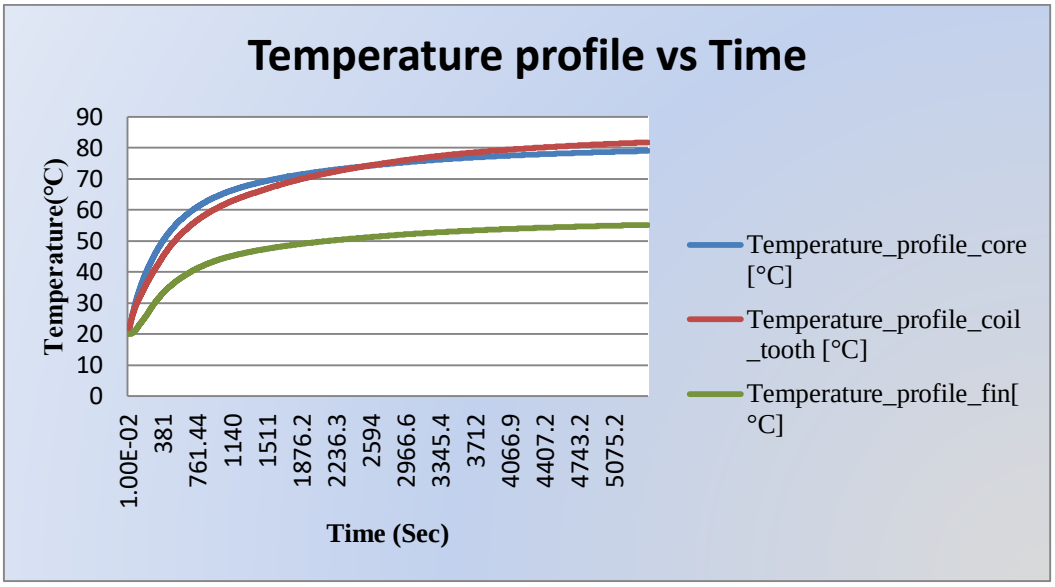

Fig. 12 Comparative graph showing temperature at various sections for a computation time of 5400 seconds

IV. CONCLUSIONS

From the comparative study it is clear that

The air current is well in the limits of (3-10 m/s) for speed 60, 75, 90, 110, 130 km/h. For the train speed of 160, 190, 200 km/h, the air current goes little above the best conditions for the actuator. This is due to ignorance of the complex parts in the geometry. The interaction of the air current with other parts of the bogie will result in the loss of kinetic energy of the molecules, thus acquiring the speed well near the best limits. For the train speed of 60, 75, 90 and 110 km/h variation of the speed from the mean speed is negligible. For the speed above 110 km/h the region near the vicinity where probe measures (y = 0.2m) deviates from the mean speed but the rest of the actuator undergoes same speed i.e. same force convective coefficient. Thus, according to the geometric constraints of the Indian coaches the actuator is physically applicable in our system and fluent analysis proves the feasibility in LHB coaches.

From the transient thermal study one can say that the temperature in the core is at a higher level as compared to coil-tooth until 2500 seconds. This is due to the variation in the temperature profile of coil, heat generation and variation in thermal conductivity in x, y and z direction.

All the geometric constraints of the LHB-FIAT rail model as well as Korean model were juxtaposed. Air current around the actuator being the critical parameter for the performance were recorded for Indian rail vehicle at different range of speed and results were promising as the air current around the actuator was found to be in the range of 3-14 m/s.
The result of the 2-D thermal simulation juxtaposed the results of the 3-D actuator not only validates the model but reduces the computation time too.
As far as future scope is concerned:
Since, the results from the fluent analysis are promising as far as the Indian Railways is concerned; further study can be done on the implementation of the actuator in the system. This thesis was concerned with a particular type of rail vehicle i.e. Rajdhani and Shatabdi. Hence, further research can be done on other class of vehicles. Further optimization of fins can be done so as to enhance the performance of the actuator. New controller strategies can be developed to determine the actuating force so as to reduce error and in return increase the ride comfort and ride quality of the vehicle. The current actuator is based on the maximum actuating force of 7700 N. This can be increased by further study.

REFERENCES:

[1] Kaloop, M. R.; Hu, J. W.; Elbeltagi, E., "Evaluation of high-speed railway bridges based on a nondestructive monitoring system." Appl. Sci. 2016, 6, 24.
[2] Orvnäs, A.; Stichel, S.; Persson, R., "Ride comfort improvements in a high-speed train with active secondary suspension." J. Mech. Syst. Transp. Logist. 2010, 3, 206–215.
[3] RDSO, "Revision and Standardization of Observation/ Measurement of Accident Investigation/Inquiry."
[4] Wang, P.; Li, H.; Zhang, J.; Mei, T., "An analytical design approach for self-powered active lateral secondary suspensions for railway vehicles." Veh. Syst. Dyn. 2015, 53, 1439–1454.
[5] Foo, E.; Goodall, R., "Active suspension control of flexible-bodied railway vehicles using electro-hydraulic and electro-magnetic actuators." Control Eng. Pract. 2000, 8, 507–518.
[6] Goodall, R.; Freudenthaler, G.; Dixon, R., "Hydraulic actuation technology for full-and semi-active railway suspensions." Veh. Syst. Dyn. 2014, 52, 1642–1657.
[7] Goodall, R.; Pearson, J.; Pratt, I., "Actuator Technologies for Secondary Active Suspension on Railway Vehicles." In Proceedings of the International Conference on Speedup Technology for Railway and Maglev Vehicles, Yokohama, Japan, 1993; 1993.
[8] Karimi, H. R., "Optimal vibration control of vehicle engine-body system using har functions." Int. J. Control Autom. Syst., 2006, 4, 714.

[9] Martins, I.; Esteves, J.; Marques, G.D.; da Silva, F. P., "Permanent-magnets linear actuators applicability in automobile active suspensions." IEEE Trans. Veh. Technol. 2006, 55, 86–94.

[10] Yoon, J. H., Kim, D., Park, N. C., Park, Y. P., "Design of a Tubular Permanent Magnet Actuator for Active Lateral Secondary Suspension of a Railway Vehicle." MDPI journals, 2017

[11] Sharma, S. K., Kumar, A., "Ride comfort of a higher speed rail vehicle using a magnetorheological suspension system." Proc. of the Inst. of Mech. E, Part K: Journal of Multi-Body Dynamic, 2017

[12] Wang, P., Mei, T. X., Zhang, J., Li, H., "Self powered active lateral secondary suspension for railway vehicles." IEEE Trans. On Veh. Tech., 2015

[13] Kim, H. C., Shin, Y. J., You, W., Jung, K. C., Oh, J. S., Choi, S. B., "A ride quality evaluation of a semi-active railway vehicle suspension system with MR damper: Railway field tests." Proc. of the Inst. of Mech. E, Part K: Journal of Multi-Body Dynamics, 2016

[14] Mellado, A. C.; Casanueva, C.; Vinolas, J.; Giménez, J. G., "A lateral active suspension for conventional railway bogies." Veh. Syst. Dyn. 2009, 47, 1–14.